

Integrated Optical Waveguide Device for Picosecond Pulse Compression

M.J.R. Heck (1), E.A.J.M. Bente (1), Y. Barbarin (1), H.D. Jung (1), Y.S. Oei (1), R. Nötzel (1), D. Lenstra (2) and M.K. Smit (1)

1) COBRA Research Institute, Technische Universiteit Eindhoven, Postbus 513, 5600 MB Eindhoven, the Netherlands, m.heck@tue.nl

2) Dept. of Electrical Engineering, Mathematics and Computer Science, Technische Universiteit Delft, the Netherlands

Abstract: We report on the fabrication and characterization of a new device, named IRIS. It is designed to increase the coherent optical bandwidth of a picosecond pulse train for subsequent pulse compression. The IRIS device consists of a concatenated array of semiconductor optical amplifiers and saturable absorbers. It is realized in the InP/InGaAsP material system for the 1550 nm range.

Measurements on the realized IRIS devices show increased broadening of the pulse spectrum as compared to an SOA of equivalent length and a smoother optical power spectrum. Consequent compression of the chirped pulses using standard single mode fiber shows decreased pulse pedestals as compared to an SOA, indicating increased linearity of the chirp. Pulse compression up to 50 % is observed.

Introduction

Trains of picosecond optical pulses with wavelengths around 1550 nm generated by semiconductor lasers have many applications, most notably in high-speed optical time division-multiplexed multiplexed (OTDM) systems [1]. Future 640 Gbit/s and Tbit/s systems will even require pulses with sub-picosecond duration. Integrated mode-locked semiconductor laser sources (MLLs) are typically able to generate transform limited pulse trains with durations down to a few picoseconds [2]. Further pulse compression can for example be obtained using soliton effects in fiber amplifiers and the subsequent use of dispersive fibers [3]. However these are bulk components.

For reasons of compactness, stability and cost, integration of a pulse compressing system with the pulse source is preferable. Several options have been proposed as an integrated optical pulse compressor. In [4] a waveguide device with concatenated semiconductor optical amplifiers (SOAs) and saturable absorbers (SAs) has been simulated and it was shown to be able to compress initially transform limited picosecond pulses. Chirped, or non-transform limited, pulses can be compressed further using integrated pulse compressing devices [5, 6].

Chirping or adding bandwidth to an initially transform limited pulse can be done using SOAs, though the amount of spectral broadening is limited and the power spectrum shows a modulation [7]. The latter will result in pulse pedestals or even satellite pulses when the pulses are compressed. In [7] we showed experimentally that an integrated optical waveguide device consisting of multiple equal SOA/SA pairs,

which we named IRIS (Integration of Regeneration, Isolation and Spectral Shaping), seems promising for abovementioned application. Compared to a single SOA the obtained bandwidth after picosecond pulse propagation through the device is larger and showed significantly less modulation in the spectrum for specific operation conditions.

In this work we study this IRIS device with respect to both its temporal pulse shaping and spectral shaping effects on a picosecond pulse train. A number of configurations of IRIS devices have been realized by us. We experimentally compare the performance of these devices with an SOA of the same length.

IRIS device design and realization

The IRIS device consists of a series of equal pairs of one SOA section and one SA section, as schematically depicted in Fig. 1(a). Its most important feature is that the saturation energy of the SA is lower than the saturation energy of the SOA. As a result a picosecond pulse that is being amplified by the device will first saturate the SA and only after that the SOA, much like in passive mode-locking.

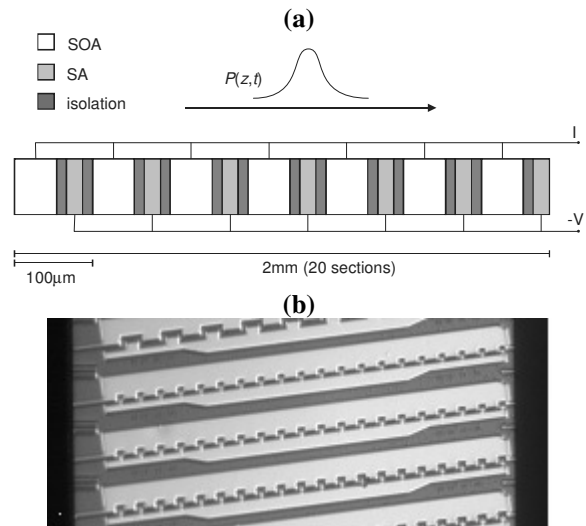


Fig. 1: (a) Schematic overview of the IRIS configuration. An input pulse (denoted by $P(z,t)$) enters from the left side, entering an SOA and exiting from the right-hand side. The ratio of the SOA and SA length within the 100 μm section (only 7 out of 20 shown) is varied. Common contacts are used for applying the injection current I and the reverse bias V . (b) Photograph of a number of realized devices, showing different configurations.

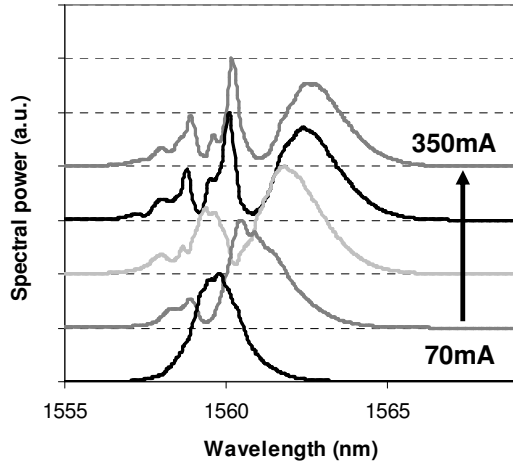


Fig. 2: Optical pulse spectra obtained after propagation through a 2 mm SOA, using a 10 GHz input pulse train with 2.0 ps duration and 0.1 W peak power. Spectra for different SOA injection currents are given.

Such devices have been realized using InP/InGaAsP bulk gain material, operating at wavelengths in the region of 1.55 μm . The sequence of SOAs and SAs is fabricated by first etching a shallow ridge waveguide of 2 μm width in the bulk gain material. To suppress lasing, the waveguide is oriented at the Brewster angle for the fundamental waveguide mode with the facets. The facets have also been antireflection coated. To create electrical isolation between the SOAs and SAs, the most highly doped part of the p-cladding layers is etched away using a dry RIE etch process. The isolation section between the SOA and SA has a length of 10 μm to 15 μm . Two gold metal pads alternately contact the waveguide sections to create two common contacts for the SOAs and SAs respectively as can be seen in Fig. 1(b). Amplification and absorption are realized by a forward or reverse electrical bias of the diodes respectively.

We have designed and realized a number of different device configurations with 20 SOA/SA pairs and varying length ratio between the SOA and SA, with the SA length increasing from 10 μm up to 20 μm . We have added 2 mm long SOAs on the same chip for reference purposes. The fabrication technology of the IRIS device is compatible with the technology to fabricate MLLs [8] or pulse shapers [5]. This allows for further integration of these components with the IRIS device.

Experimental results

A picosecond pulse train propagating through an SOA or SA experiences a self-phase modulation (SPM) due to the effects of gain saturation, carrier heating and other ultrafast nonlinear refraction [9]. The result of this SPM is a change in the optical spectrum of the pulse train. This effect increases the bandwidth of the spectrum of a pulse train, effectively chirping it. Depending on the shape of the chirp profile, the pulses can be compressed conse-

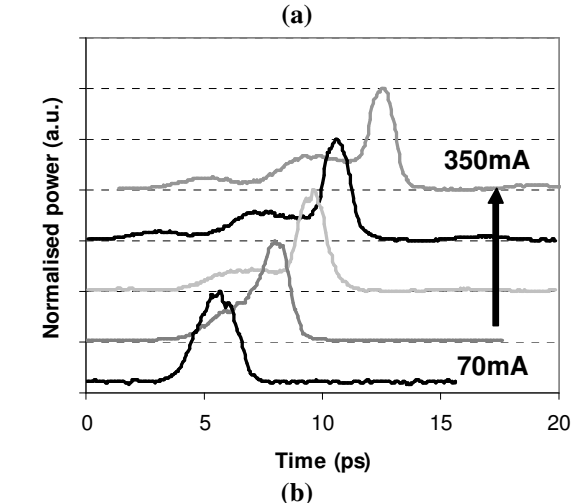


Fig. 3: (a) Temporal pulse profiles, corresponding to the spectra shown in Fig. 2, after propagation through 15 m of SMF. Profiles have been horizontally shifted for easy comparison. The temporal profiles have been obtained with a 700 GHz optical sampling oscilloscope. In (b), a trace obtained at 350 mA injection current is shown. The zero level (horizontal) trace is due to the pulsed injection current. Jitter in the pulsed laser and sampling laser in the oscilloscope cause the broadening of the pulse profile trace.

quently by a dispersive element.

We have measured spectra of short optical pulses that have propagated through IRIS devices with SA lengths of 10 μm and 20 μm (see Fig. 1(a)). A 10 GHz pulse train, with pulse durations of 2.0 ps and a peak power of 0.1 W is used for the input. Also we have measured temporal pulse profiles exiting from the IRIS devices. For this we use a 700 GHz bandwidth optical sampling oscilloscope. A lensed fiber tip is used for coupling the pulse train in and out of the IRIS device and a total of 15 m of standard single mode fiber (SMF), with a dispersion of 18 ps/nm/km, is used in between the device and the sampling oscilloscope. For comparison spectra and pulse shapes are also obtained for pulse train propagation through a 2 mm SOA, i.e. with an equivalent total length to the IRIS device. Pulsed injection current (300 ns pulses, 1 % duty cycle) is used to prevent heating of the device.

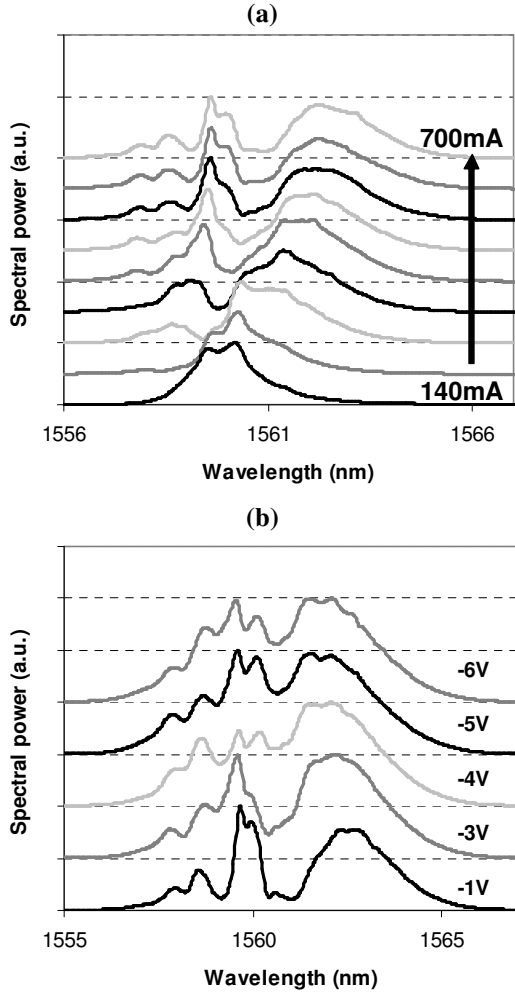


Fig. 4: Optical pulse spectra obtained after propagation through an IRIS device with $10\ \mu\text{m}$ SAs, using a $10\ \text{GHz}$ pulse train with $2.0\ \text{ps}$ duration and $0.1\ \text{W}$ peak power. **(a)** Total injection current for the $20\ \text{SOAs}$ is varied. The SA reverse bias voltage is $-1\ \text{V}$. **(b)** Injection current is fixed at $700\ \text{mA}$, SA bias voltage is varied from $-1\ \text{V}$ down to $-6\ \text{V}$.

In Fig. 2 pulse spectra after propagation through a $2\ \text{mm}$ SOA are presented for different injection currents. As can be seen, increasing the injection current introduces a shift of the spectrum towards longer wavelengths, as can be expected from the gain saturation [9]. However the spectral profile shows much structure, with peaks around the wavelength of the input pulses at $1560\ \text{nm}$. This indicates that the induced chirp profile over the pulse train is not linear. Therefore pulse compression using mainly second order dispersion, as introduced by e.g. SMF, is not optimal. We have measured the temporal output pulse shapes after propagation through $15\ \text{m}$ of SMF, with a total dispersion of $0.34\ \text{ps}^2$. This corresponds approximately to a pulse broadening (or compression) value of $0.3\ \text{ps}$ per nanometer optical bandwidth, assuming linear chirp profiles. Given the optical bandwidths as mentioned in Fig. 2, this value of the dispersion will clearly show either pulse compression or broadening, depending on the sign of the chirp of the pulses. As a result, applying this amount of dispersion gives qualitative insight in the shape of

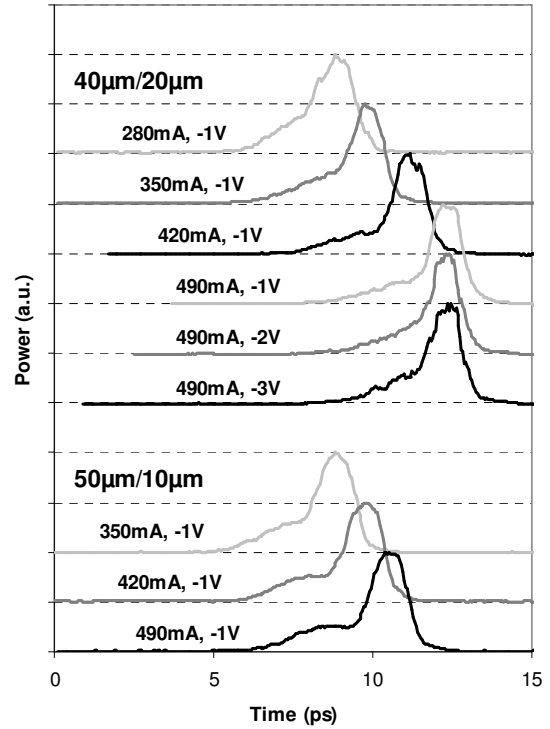


Fig. 5: Normalized temporal pulse profiles after propagation through $15\ \text{m}$ of SMF, obtained with a $700\ \text{GHz}$ optical sampling oscilloscope. Profiles have been horizontally shifted for easy comparison. Pulse profiles for IRIS devices with $20\ \mu\text{m}$ SAs ($40\ \mu\text{m}$ SOAs) and $10\ \mu\text{m}$ SAs ($50\ \mu\text{m}$ SOAs) are given, for various SOA injection currents and SA bias voltages.

the phase profile over the pulse. We note that a full phase characterization of the pulse can be made using the method mentioned in [10], using only the temporal pulse profile and the optical power spectrum.

Fig. 3 shows the obtained temporal pulse shapes. As can be seen the pulse is only partially compressed at the higher injection currents, with one or two weaker and longer pulses preceding the compressed part.

In conclusion it can be said that the SOA is not a suitable device for chirping an optical pulse with the aim of further pulse compression. As the chirp profile is not linear, using only second order dispersion, e.g. by a SMF, will only partially compress the pulses. Also, due to the modulation in the optical spectrum, even more advanced pulse compressors, e.g. as mentioned in [5], can not avoid the generation of satellite pulses when trying to fully compress the pulse.

In Fig. 4(a) spectra observed from pulses after propagation through an IRIS device with $10\ \mu\text{m}$ SAs are given. As the $20\ \text{SOAs}$ have a common contact, the total injection current is given. The SAs are reversely biased with a voltage of $-1\ \text{V}$. As can be seen, the spectrum is still heavily modulated at the higher injection currents. However, increasing the voltage over the SAs severely decreases this modulation depth, as can be seen in Fig. 4(b). Again, because of the $15\ \text{m}$ SMF, a second order dispersion of $0.34\ \text{ps}^2$ is applied to the pulse train after propagation through the IRIS devices. Fig. 5 shows the obtained temporal

pulse profiles. Comparing the pulse profiles obtained with IRIS devices with those obtained by an SOA (Fig. 3) shows that the pulse pedestal and preceding pulses decrease. This effect is more pronounced for the IRIS devices with 20 μm SAs as compared to those with 10 μm SAs. Also, increasing the bias voltage over the SAs decreases the pedestal even more. The obtained compression is almost 50%, with output pulse durations down to 1.1 ps for IRIS devices with 20 μm SAs at higher injection currents. This value of the pulse duration is close to the measurement limitation of the 700 GHz sampling oscilloscope due to the limited risetime.

The spectral bandwidth of over 4 nm (Fig. 4(b)) allows for further pulse compression, either by optimizing the SMF length of by adding higher order dispersion. This depends on the exact shape of the chirp profile of the pulses.

Concluding it can be said that the chirp profile of a train of pulses with a duration of 2.0 ps after propagation through an IRIS device makes it possible to compress these pulses further using second order dispersion. A total dispersion of 0.34 ps^2 compresses these pulses down to 1.1 ps, i.e. almost 50%.

Conclusion

We have fabricated a device, named IRIS that is able to chirp a train of picosecond pulses. Measurements show that pulses with an initial duration of 2.0 ps can be compressed down to 1.1 ps after propagation through the device, using only second order dispersion, without the appearance of leading or trailing pulses. This indicates a good linearity of the chirp over the pulses. Such compression is not possible using an SOA of the same length as the obtained chirp profile is less linear and only partial compression of the pulses occurs. This is an important result as second order dispersion is the dominant dispersion term in SMF, but also in integrated dispersive components [6].

The shape of the spectrum obtained has a more smooth structure as compared to that from an SOA. This makes the IRIS device more suitable for use in combination with an arbitrary pulse shaper [5] as the spectrum needs less power equalization.

As the fabrication technology of the IRIS device is compatible with both MLLs [8] and pulse shaping devices [5], it is a promising candidate for further integration to create monolithically integrated (sub-) picosecond or arbitrarily shaped pulse sources.

Acknowledgments

This research is supported by the Towards Freeband Communication Impulse of the technology programme of the Dutch Ministry of Economic Affairs and by the Dutch NRC-Photonics programme.

References

- 1 L.A. Jiang et al., *J. Opt. Fiber. Commun. Rep.* 2, pp. 1-31, 2005
- 2 R. Kaiser et al., *IEEE Photon. Technol. Lett.*, vol. 15, no. 5, p. 634, 2003.
- 3 J.T. Ong et al., *IEEE J. Quant. Electr.*, vol. 29, no. 6, p. 1701, 1993
- 4 Shimizu et al., *Jpn. J. Appl. Phys.*, vol. 39, p. 475, 2000
- 5 M.J.R. Heck et al., *ECIO*, p. 351, 2005
- 6 Y. Lee, *Appl. Phys. Lett.*, vol. 73, no. 19, p. 2715, 1998
- 7 M.J.R. Heck et al., *IEEE/LEOS Benelux*, p. 41, 2006
- 8 Y. Barbarin et al., *Opt. Expr.*, vol. 14, p. 9716, 2006
- 9 J.M. Tang and K.A. Shore, *IEE Proc.-Optoelectron.*, vol. 146, p. 45, 1999
- 10 M. Hacker et al., *Opt. Expr.*, vol. 9, no. 4, p. 191, 2001